European Journal of Radiology 88 (2017) 155–162

Contents lists available at ScienceDirect

European Journal of Radiology

journal homepage: www.elsevier.com/locate/ejrad

Whole-body MRI in children: Would a 3D STIR sequence alone be sufficient for investigating common paediatric conditions? A comparative study

Laura Merlini [a,*], Marc Carpentier [b], Solène Ferrey [a], Mehrak Anooshiravani [a], Pierre-Alexandre Poletti [c], Sylviane Hanquinet [a]

[a] Department of Radiology, Unit of Pediatric Radiology, University Hospital Rue Willy-Donzé 6, 1205 Geneva, Switzerland
[b] Department of Epidemiology, University Hospital, Rue Gabrielle-Perret-Gentil 4, 1205 Geneva Switzerland
[c] Department of Radiology, University Hospital, Rue Gabrielle-Perret-Gentil 4, 1205 Geneva, Switzerland

ARTICLE INFO

Article history:
Received 2 August 2016
Received in revised form 1 November 2016
Accepted 17 January 2017

Keywords:
Children
Whole-body magnetic resonance imaging
3D short tau inversion-recovery sequence
Accuracy

ABSTRACT

Objectives: To test the performance of a single 3D IR T2-Weighted sequence compared to a Whole-body MRI protocol including DWI, T1-Weighted and STIR 3D IR (3S) in a pediatric population.
Methods: Two radiologists (15 and 30 years of experience),reviewed WBMRIs: first the STIR alone and 2 weeks later the 3S protocol. The indications were variable. Only positive findings were explicitly reported. A third reader compared the results to gold standard (GS) exams specific for the pathology. Agreement between the two readers, sensitivity and positive predictive value of STIR were calculated.
Results: fifty-four WBMRIs were included (16 suspected child abuse, 8 chronic recurrent multifocal osteomyelitis (CRMO), 11 lymphomas, 4 osteosarcomas, 9 neuroblastomas, 6 histiocytosis). The mean age was 6 years 10 months, range: 1 month to 15 years.

Agreement between readers was of 0.87 [0.82–0.91] for 3D STIR, and 0.89 [0.83–0.93] for the 3S protocol. For reader 1 sensitivity of 3D STIR was 81.6% and of 3S 81.0%. For reader 2 it was 74.1% for 3D STIR and 74.7% for 3S. For both readers and for both protocols, the positive predictive value (PPV) depended on the type of disease (for example 100% histocytosis and osteosarcomas, >90% for child abuse, >85% CRMO but <70% for lymphoma and neuroblastoma).
Conclusions: Sensitivities were not different between the 2 protocols, for each reader and were different between the 2 readers for each protocol.

1. Introduction

Whole-body magnetic resonance imaging (WB-MRI) is widely used as a non-radiating screening exam in a variety of paediatric diseases including malignancies [1–8] due to the many inherent advantages compared to other imaging modalities, such as the absence of ionizing radiation [9,10] and its high tissue contrast. However, there are some obstacles for its practical application and among them is the relatively long study time. Many papers in the recent literature suggest to find abbreviated MRI protocol with the same accuracy as multi-sequence ones in order to reduce the study time and increase patient comfort even in adults [11–14]. This is even more necessary in children: reduction of the sedation time in younger patients will not only decrease sedation-related risks, but also overall costs. The most frequently used single sequence for a fast study in current practice is the 2D fast turbo short tau inversion-recovery (STIR) coronal sequence [15–18]. According to the literature, this sequence is reported as fast and highly sensitive for the detection of lesions in multiple diseases but insufficient in detecting lung metastasis [17] as well as lesions in other areas such as ribs and scapula [8,19]. Most institutions use additional sequences such as diffusion-weighted imaging with fat suppression (DWI) [2,20–22] and T1-weighted sequences which is considered as the cornerstone of bone marrow imaging both in cancer and rheumatologic disorders [23,24].

Since 2010, in our department we have been using a whole-body MRI protocol that includes three sequences: T1-weighted, IR DWI and, to replace the widely used 2D STIR sequence by a 3D T2-weighted inversion-recovery sequence (3D STIR). The latter combines properties of fat-saturated T2-weighted images with a better spatial resolution of lesions due to a large anatomical coverage as well as the ability to slice through the volume of interest and a

* Corresponding author.
E-mail address: laura.merlini@hcuge.ch (L. Merlini).

http://dx.doi.org/10.1016/j.ejrad.2017.01.014
0720-048X/

Table 1
Sensitivities.

Disease (N = 46)	Reader 1		Reader 2	
	3D STIR	3S	3D STIR	3S
Child abuse s. (N = 13)	62.2% (28/45)	62.2% (28/45)	44.4% (20/45)	51.1% (23/45)
CMRO (N = 8)	89.7% (44/49)	85.7% (42/49)	77.5% (38/49)	71.4% (35/49)
Histiocytosis (N = 4)	100% (6/6)	100% (6/6)	100% (6/6)	100% (6/6)
Lymphoma (N = 11)	86.2% (25/29)	86.2% (25/29)	86.2% (25/29)	86.6% (26/29)
Neuroblastoma (N = 6)	91.8% (34/37)	94.5% (35/37)	94.5% (35/37)	97.2% (36/37)
Osteosarcoma(N = 4)	62.5% (5/8)	62.5% (5/8)	62.5% (5/8)	50%(4/8)
Total	81.6%(142/174)	81.0% (141/174)	74.1%(129/174)	74.7%(130/174)

Comparison of Sensitivities between 3D STIR sequence and the whole protocol (3S) per Reader and per disease. The first number in bracket is the number of lesions recognized by the reader with the protocol and the second is the number of lesions recognized by the gold standard.

sufficiently high resolution (isotropic voxel size = 0.9–1 mm^3) [25]. Moreover, the possibility to perform axial reconstruction could increase recognition of flat bone lesions [8,19].

However, a study including all these sequences may take 45/70 min, quite long for children and requires a long sedation for younger children while older children are requested to tolerate and hold still for long MR studies.

The aim of our study was to investigate if the 3D STIR alone is not inferior to the complete protocol including all three sequences (3S). If this is the case, we would be able to propose a faster 20-min study, with significant increase in patient comfort and decrease in sedation time, which is highly desirable in paediatric practice.

2. Material and methods

The institutional review board (CER:13-073R) approved this retrospective study and waived the need to obtain informed consent.

We reviewed clinical charts of children who underwent WB-MRI in the paediatric radiology unit between March 2013 and March 2015. We only included patients for whom diagnostic techniques validated by the literature as the gold standard (GS) for the specific disease were performed and in whom a clinical follow-up was available. We thus considered: neuroblastoma cases who had undergone ^{131}I-meta-iodobenzylguanidine (MIBG) scintigraphy; lymphoma and osteosarcoma patients who had 18F-fluoro-2-deoxy-D-glucose positron emission tomography (FDG-PET)/computed tomography (CT), chronic recurrent multifocal osteomyelitis (CRMO) cases with technetium-99 m scintigraphy, and cases of child abuse who had a skeletal X-ray survey, abdominal and/or soft tissues ultrasound; and for histiocytosis, patients with skeletal X-ray survey or technetium-99 m scintigraphy. We did not include patients with incomplete GS, for example if bone scintigraphies, MIBGs or PETs did not include the entire lower limbs.

GS exams were performed within an interval of 1–10 days for all diseases except for patients with suspected child abuse in whom all exams were performed the same day as WB-MRI.

2.1. MRI protocol

All studies were performed on a 1.5 T Avanto MR scanner (Siemens, Erlangen, Germany). The patients were imaged with a phased array coil, from head to heels, under free-breathing. None of the patients had contrast or antiperistaltic agent injection. All children under the age of 6 years underwent sedation.

Body coverage was achieved usually with two or three stations. The following sequences were performed:

1) Coronal 3D STIR (SPACE): TR 2000 TE 174/284 ms, TI 160 ms, Turbofactor 85, BW 446 kHz, FOV 448 × 448 mm, matrix size 300 × 320, parallel acceleration factor 2, variable flip angles along the echo train, slice thickness 1.3 mm, N° signals averaged 1. For each patient, thin Maximum Intensity Projection (MIP) and multiplanar reconstruction were performed. The average time was 20 min and the range was 6/26 min depending on the number of body stations which varies according to the child size.
2) Coronal T1 –Weighted FSE: TR/TE 554/11 ms, ETL 2, BW 150 kHz, slice thickness 5 mm with 1 mm gap, matrix 270 × 384, FOV 400 × 400 or in function of the patient size, angle 180, N° signals averaged 2. The average time was 10 min and the range was 6/16 min depending on the number of body stations.
3) Axial DWI STIR-EPI. TR/TE 8400/72 ms, TI 160 ms, slice thickness 4 mm with multiple signal averages, slice gap 0, matrix 148 × 184, FOV 360 × 360 or in function of the patient size,
4) acquired on 3 orthogonal directions. ADC maps were calculated in-line by the MRI scanner with b = 0 and 600. Acquisition was in the axial plane and then reformatted in the coronal plane using b = 600. The average time was 15 min and the range was 12–20 min depending on the number of body stations which varies according to the child size.

The number of coil stations and parameters were determined by the radiologist to optimize the study for each patient. The average study time for the three sequences was 50/70 min.

Seamless coronal whole-body images were obtained by merging of separate acquired stations. DWI was displayed in inverted grey scale intensity on a 20 mm coronal MIPs image (PET-like).

2.2. MRI interpretation

The first author (L.M.) anonymized all MRI studies, which were coded and transferred to a dedicated computer station and stored in random order. All studies were examined with OsiriX MD v 3.0.2 software (Geneva, Switzerland). Osirix can display coronal volumetric data and reformatted images in the axial and sagittal planes and also reorient the dataset by rotation around the chosen points.

Two paediatric radiologists (S.F. and S.H., with 15 and 30 years of paediatric radiology experience and MRI) and the first author (L.M. 15 years of experience) performed a training session together on 5 whole-body MRI studies, one normal and 4 with several diseases (multimetastatic neuroblastoma, non accidental trauma, neurofibromatosis type I, chronic recurrent multifocal osteomyelitis) which were not included in the series, in order to agree on assessment criteria for "lesions" of bone, soft tissues and solid organs.

The two readers independently evaluated two separate sets in a fixed order: first only 3D STIR images of all patients, on coronal, axial and sagittal reconstructions and then, 2 weeks after the first reading, the whole protocol (3S) including the three sequences 3D STIR, T1-W and fat sat DWI (3S) for the same patients. They evaluated the composed whole-body images but all native data were also available if needed (non reconstructed). Readers were blinded for all clinical and radiological data: in particular they were not aware of the type of pathology or clinical indication. Each observer reg-

Table 2
Positive Predictive Value.

Disease	Reader 1		Reader 2	
	3D STIR	3S	3D STIR	3S
Child abuse s. (N = 13)	93.3 (30/28)	93.3 (30/28)	90.9 (22/20)	92.0 (25/23)
CMRO (N = 8)	86.3 (51/44)	97.7 (43/42)	97.4 (39/38)	92.1 (38/35)
Histiocytosis (N = 4)	100.0 (6/6)	100.0 (6/6)	100.0 (6/6)	100.0 (6/6)
Lymphoma (N = 11)	62.5 (40/25)	59.5 (42/25)	69.4 (36/25)	55.3 (47/26)
Neuroblastoma (N = 6)	68.0 (50/34)	62.5 (56/35)	68.6 (51/35)	62.1 (58/36)
Osteosarcoma(N = 4)	100.0 (5/5)	100.0 (5/5)	100.0 (5/5)	100.0 (5/5)
Total (N = 46)	78.0(70.9; 86.1)	77.5(68., 87.1)	81.1(73.0; 91.8)	73.0(62.7; 84.9)

Comparison of Positive Predictive Value (PPV) between the 3D STIR sequence and the whole protocol (3S) per Reader and per pathology. The first number in brackets indicates the lesions found by the reader and the second the "true lesions" among them confirmed by the gold standard.

Table 3
Pairwise comparisons.

	Reader 1 3D STIR	Reader 1 3S	Reader2 3D STIR	Reader 2 3S
Sensitivities:	81.6 (70.7; 89.7)	81.0 (70.0; 89.3)	74.1 (60.0; 85.4)	74.7 (60.6; 85.8)
Differences between protocols	0	−0.6 (−4.1; 2.2)		
			0	0.6 (−8.6; 8.5)
Differences between readers	0		−7.4 (−15.2; −1.2)	
		0		−6.3 (−15.2; 0.0)

Pairwise comparisons of overall estimations and 95% confidence interval of sensitivities between protocols for each rater, and between raters for each procedure. The non inferiority in sensibility of 3D STIR alone compared with 3D protocol is proved for reader 1 (difference in sensibility null or inferior than 5%) but not for reader 2 (difference in sensibility more than 5%).

istered the reading time for the whole-body MRI data with the 3D STIR protocol as well as for the whole protocol separately. Only positive findings were explicitly reported (free-response framework).

Presence of abnormalities was recorded for the following predefined categories:

Lymph nodes were considered as positive if their short-axis diameter exceeded 10 mm.

Extranodal locations and solid organs were considered independently of the size or pathological signification: as an example a neuroblastoma was considered as "mass".

Soft tissue involvement was considered as a lesion when isolated and not when associated to fractures, osteomyelitis or other abnormalities.

Joint effusion was considered as a lesion when it was more than physiological, according to the reader's experience.

Two abnormalities (ex. metastasis) on the same anatomical structure (ex. liver or bone) were considered as one lesion.

IR DWI were interpreted according to literature data [20,26]: high signal intensity in brain, salivary glands, tonsils, spleen, gallbladder, adrenal glands, prostate, testes penis, endometrium, ovaries, spinal cord, peripheral nerves and bone marrow was considered as physiological. Apparent diffusion coefficient (ADC) maps were performed but measurements were not used for disease detection.

Then, the first author solved location or tagging problems and asked the readers to better specify lesions when needed: for example "radial lesion" indicated as "radial head lesion" or " sixth thoracic vertebral body lesion" was in fact "seventh" due to the difficulty to count vertebral bodies etc.

To measure the performance of 3D STIR in comparison to 3S, the third reader compared WB-MRI to the gold standard findings.

2.3. Statistical analyses

Statistical analyses were done with CRAN R version 3.2.0. Concordance between readers was calculated for each protocol (3D STIR and 3S) with the free-response kappa, which accounts for the free-response framework by assuming that the number of possible abnormal ratings is very large tending to infinite [27]. This free-response kappa was computed for all the ratings of 3D STIR −sequences and 3S protocol irrespectively of the availability of a gold-standard.

Clustering was accounted for to provide adequate 95% confidence intervals. These intervals requiring a sufficient number of patients and observations, 95% confidence intervals were therefore only computed for the overall sensitivity and positive predictive value. We used a bootstrap-procedure, where the 84 clusters were sampled with replacements. The 95% confidence intervals are based on the percentile 2.5 and 97.5 of 10000 bootstrapped samples.

To compare sensitivities of each reader and technique, differences between sensitivities were computed from all bootstrapped samples and a 95% confidence interval was computed for each mean difference, between procedures for each reader, and between readers for each procedure. The non-inferiority margin of 3D STIR compared to 3D protocol was fixed at 5%.

3. Results

We retrieved 54 whole-body MRIs performed with the complete protocol that could be compared to a complete imaging study considered as gold standard (GS) for the specific pathology as explained in the Methods section. (29 males and 25 females; mean age: 6 years 10 months, range: 1 month to 15 years). Ten children were sedated. Sixteen were cases of suspected child abuse, 8 chronic recurrent multifocal osteomyelitis (CRMO), 11 lymphomas, 4 osteosarcomas, 9 neuroblastomas, 6 Langerhans cell histiocytosis.

Among patients with lymphoma, 6 were investigated with WB-MRI at presentation and 5 in the follow-up, 6 patients with neuroblastoma had WB-MRI at presentation and 3 at follow-up. All patients with osteosarcoma, CRMO and Langerhans cell histiocytosis were investigated at presentation.

Among the 54 patients, 8 (3 suspected child abuse syndrome at presentation, 2 hystiocitosis and 3 neuroblastoma during the follow up) had no lesions shown by the GS technique or by WBMRI. In the other 46 patients, GS exams showed 174 lesions.

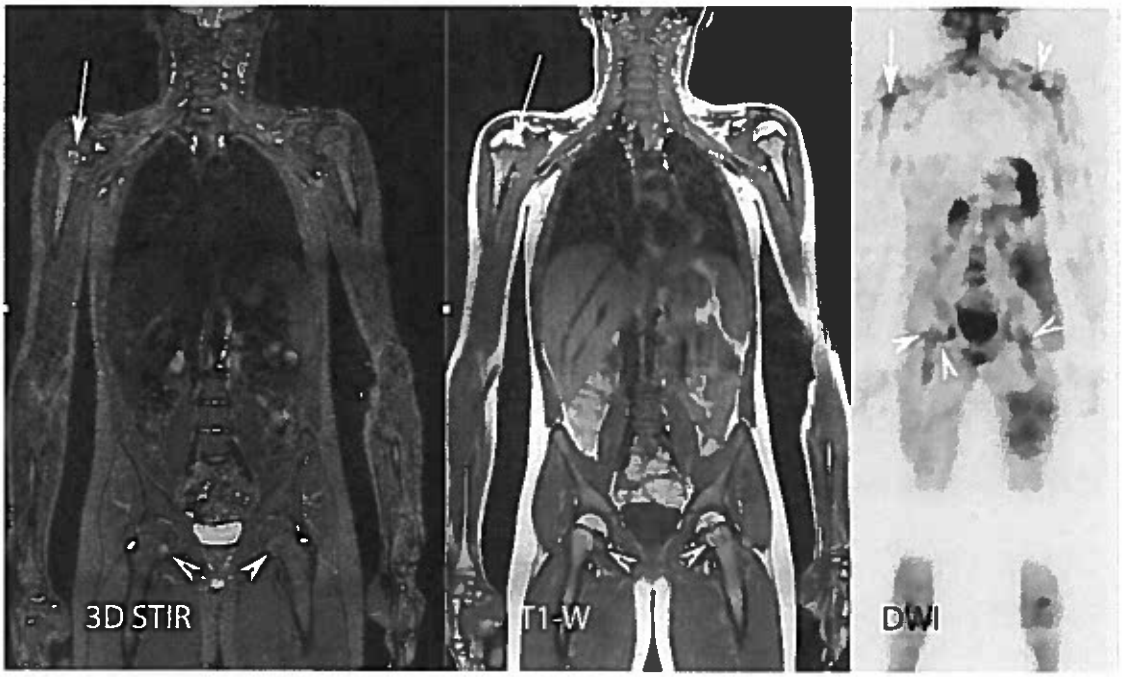

Fig. 1. Lymphoma WB-MRI.
Eleven year-old boy with lymphoma after the end of the treatment (chemotherapy): 3D STIR, T1 Weighted, and DWI show a lesion in the proximal metaphysis of the right humerus (arrows) and other small metastasis on femoral metaphysis (arrowheads)

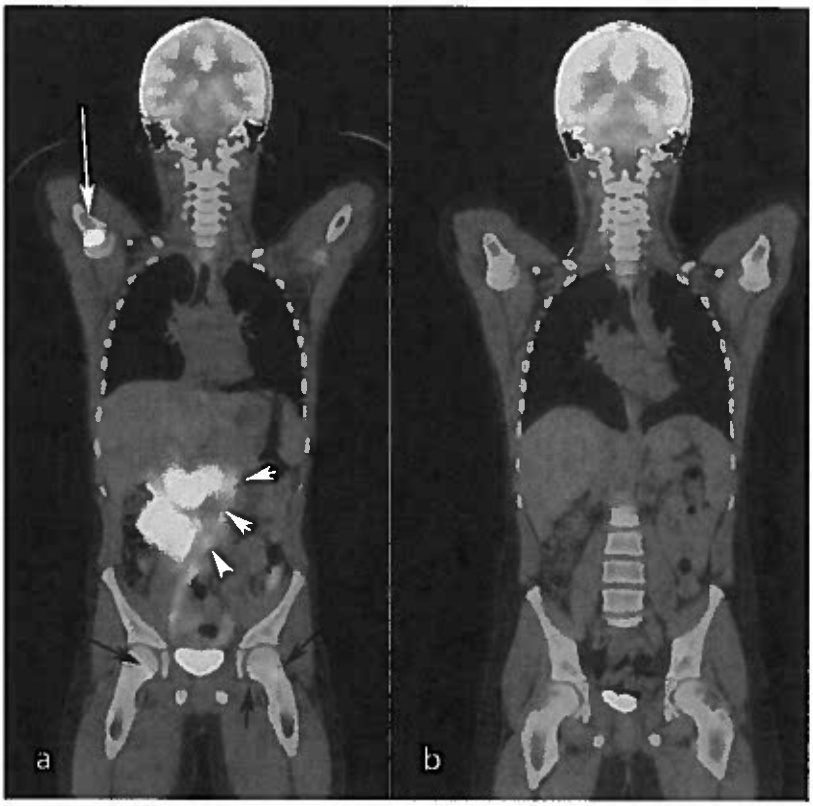

Fig. 2. a and b Lymphoma PET CT.
Same patient as in Fig. 1.a) PET CT at onset one year earlier: a large retroperitoneal mass (white small arrows), the humeral metastasis ((white large arrow) and the small femoral metastasis (black arrows). b) PET CT performed at the same time as the WB-MRI shown in Fig. 1: no lesions. The lesions persist on the WB-MRI longer than on PET CT but they are not metabolically active and can not be considered as metastatic lesions.

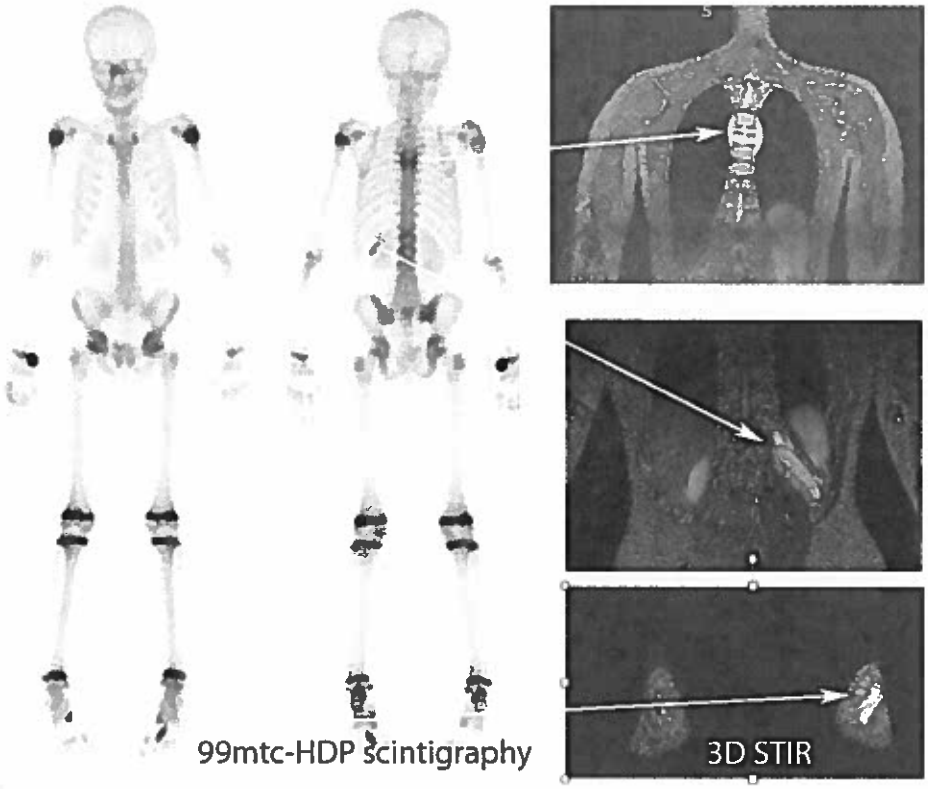

Fig. 3. Chronic Recurrent Multifocal osteomyelitis (CRMO).
Ten year-old girl at presentation for left foot pain. Scintigraphy and 3D STIR: dorsal vertebral lesion, left costal and left metatarsal lesions are shown by both techniques (long white arrows)

The mean reading time for the whole-body MRI with 3D STIR alone was 20 min for both readers. The mean recorded time for the evaluation of the 3S protocol was 32 min for reader 1 and 28 min for reader 2.

Regarding the agreement between readers, the free-response kappa was 0.87 [0.82–0.91] for 3D STIR, and 0.89 [0.83–0.93] for the 3S protocol. The difference of agreement for the two protocols (3D STIR and 3S) was calculated as 0.02 (−0.03;0.07).

Table 1 illustrate the sensitivities per protocol per reader and per disease.

Reader 1 identified 142 lesions out of 174 GS-based true lesions with 3D STIR and 141 with 3S. (Table 1) The missed lesions with 3D STIR were: 16 metaphyseal and 5 rib fractures in 5 cases of child abuse, 5 lung metastasis in lymphomas and osteosarcomas, 5 nodal localizations of lymphoma with a size inferior to one centimeter and one was a liver lesion in lymphoma. Reader 1 over diagnosed (not recognized by the GS) 40 lesions with 3D STIR and 39 with 3S (Table 2). These lesions were bone lesions of lymphoma and neuroblastoma (all on follow-up exams) bone lesions of child abuse and CRMO. In particular, reader 1 tended to over diagnose CRMO lesions with 3D STIR alone.

Reader 2 correctly described 129 out of 174 lesions with 3D STIR alone and 130 with 3S (Table 2a). The missed lesions were the same 30 as the reader 1 but she also missed more bone lesions on CRMO. Reader 2 overdiagnosed (not recognized by GS) 30 lesions with 3D STIR and 38 with 3S. The overdiagnosed lesions were the same as for reader 1 but reader 2 was slightly more precise for CRMO lesions.

PPV global estimations for 3D STIR was equivalent to 3S for reader 1 (78.0 vs 77.5) and higher (81.1) than 3S (73.0) for reader 2 even though it was not statistically compared.

For both readers, the PPV depended on the type of disease: it was 100%for histocytosis and osteosarcomas, superior to 90% for child abuse and superior to 85% for CRMO but less satisfactory for lymphomas and neuroblastomas (Table 2).

The difference of sensitivity between the 2 readers was significant with both protocols, being −7.4 (−15.2; −1.2) for 3D STIR; −6.3 (−15.2; 0.0) for 3S (Table 3).

The difference of sensitivity between the 2 protocols was close to zero for both readers (Table 3) being respectively −0.6 (−4.1; 2.2) for reader 1 and 0.6 (−8.6; 8.5) for reader 2. Considering the confidence interval, only for reader 1 there was less than the 5% of non-inferiority margin for 3D STIR in comparison to 3S; for the second reader it was more than 5% (Table 3).

4. Discussion

Our study investigated if the choice of a short protocol with 3D STIR alone changes the performance of WB-MRI compared to a protocol including multiple sequences. If we could prove our hypothesis we could achieve a significant reduction of the scanning time in order to obviate technical problems related to sedation time and lower compliance of paediatric patients.

Our findings indicate that the reading time of WB-MRI for both readers was similar to data reported in the literature [4].

The inter reader agreement was similar for the two protocols (0.87 for reader 1 and 0.89 for reader 2) and it could be considered as very good. Our results showed a better concordance than the ones reported by the only paper we found in the paediatric literature about inter observer agreement for whole-body MRI[4]. The reason of our better concordance might be that our readers were

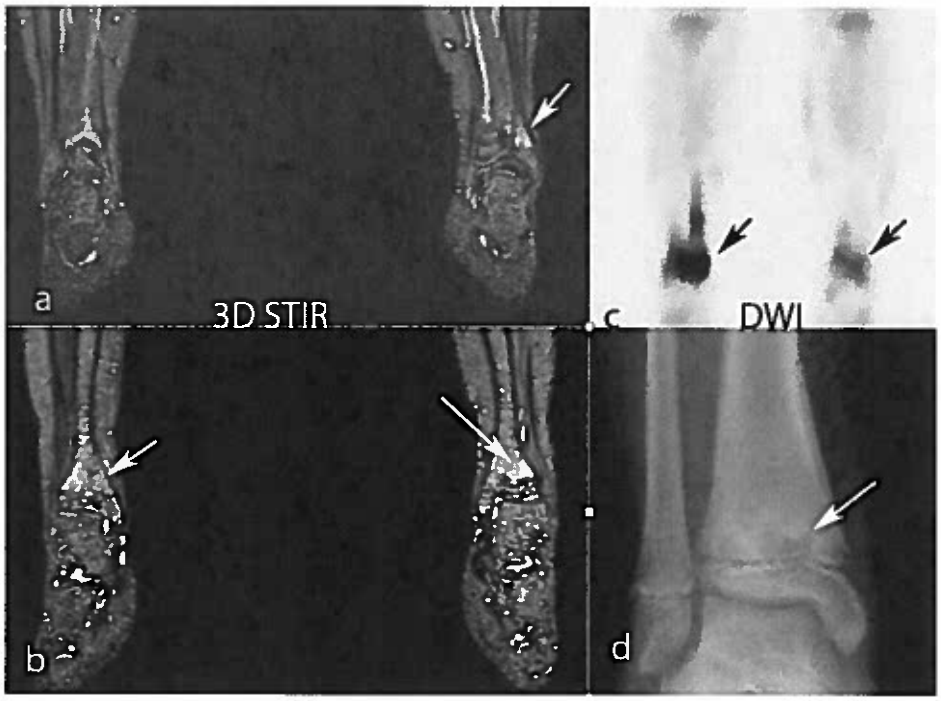

Fig. 4. Chronic Recurrent Multifocal Osteomyelitis (CRMO).
Same patient as in Fig. 3. 3D STIR (a and b) and DWI (c) show also multiple tibial and peroneal distal metaphyseal lesions not depicted by scintigraphy. These lesions became visible on XRays one month later (d).

both experimented paediatric radiologists while one of the readers in the cited study had 5 years of experience. We also used a different kappa statistic analysis suited to situations of free-response assessments where only positive diagnoses are explicitly reported. The free-response kappa offers a solution for the measurement of agreement in the free-response framework. It relies on Cohen's kappa statistics and can be interpreted the same way, as agreement beyond chance. This test should be used when one is assuming that the number of potential abnormalities is important, tending to infinite.

Analysis of the performance showed that sensitivity and PPV was significantly different for the 2 readers (reader 1 had a better sensitivity than reader 2 who had a better PPV) no matter which protocol was used (3D STIR or 3S). In other words, each reader made the same number and type of errors with the two protocols.

When comparing the sensitivity of the two protocols, we found no difference between 3D STIR and 3S for a given reader (Table 3). However, the non inferiority of 3D STIR compared to 3S could be only proved for the reader 1: in fact, for reader 1, the 95% confidence interval was inferior to the upper limit we fixed to establish the non inferiority of 3D STIR (5%) while for reader 2 the confidence of interval was superior (Table 3).

Analysis of the mistaken lesions (missed or over diagnosed in comparison to a gold standard) by both readers shows that the use of the 3S protocol does not increase the performance of the detection when they have been missed or overdiagnosed at 3D STIR alone. Therefore, the impact of the mistaken lesions (missed or overdiagnosed) on the clinical management will be the same using both protocols. This suggests that mistaken lesions are related to the intrinsic limitation of the MR technique itself, in relationship with the type of the pathology in concordance with data of the literature, rather than to the type of protocol.

As an example, it is widely accepted that WB-MRI cannot replace the skeletal survey in cases of child abuse syndrome because it is insensitive in the detection of high specificity indicators of this condition such as metaphyseal fractures [28]. On the same way, the fact that both readers did not detect most of the lung metastasis was not surprising considering recent literature data [17].

Other aspects of our findings are less well reported in the literature: for example, our study indicated that many overrated lesions were long or flat bone lesions on follow-up exams in children with lymphoma or neuroblastoma after treatment with chemo or radiation therapy. Such bone abnormalities, in presence of complete normalization of the MIBG scan or PET/CT after chemotherapy do not necessarily indicate persistence of disease but may be due to delayed normalization which can be as long as more than 2 years after the end of chemotherapy [29–31]. (Figs. 1 and 2). However, once again it has to be pointed out that the same lesions were overrated both by 3D STIR alone and 3S.

Other mistaken lesions were metaphyseal lesions of CRMO, often overrated because of the proximity to the physis that can be sometimes irregular and has the same hyperintense signal as lesions on STIR [32,33]. (Figs. 3 and 4).

However, once again it has to be pointed out that the same lesions were overrated both by 3D STIR alone and 3S.

Our study seems to indicate that the addition of DWI to conventional whole-body MRI sequences does not enhance lesion conspicuity, in contradiction with recently published results in oncological adults and children [20,22,34]. This could be related to a statistical limitation due to the small number of patients affected by neoplastic or hematologic disease and to the heterogenicity of this group, while the studies in the literature are highly homogenous mostly concerning lymphomas at initial diagnosis. Moreover, it is also possible that the efficacy of DWI is reduced in children versus adults for constitutional factors such as the low body weight and scarcity of body fat.

On the other hand other recent studies do not confirm that DWI improves the performance of whole-body MRI [1,4]. However it is known that DWI can be particularly difficult to interpret in children

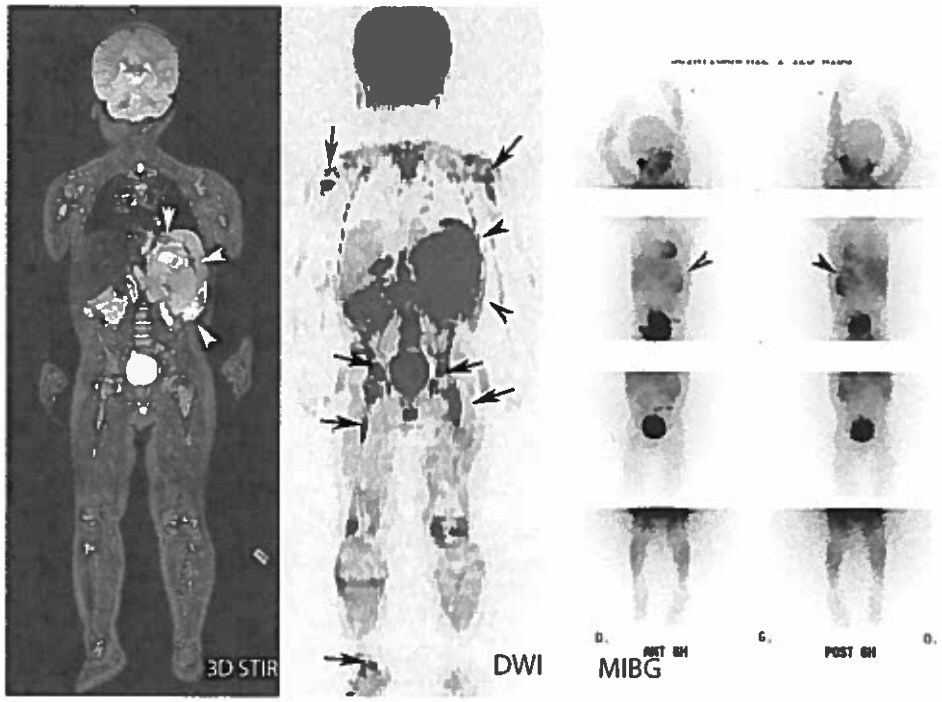

Fig. 5. Neuroblastoma.
Four year-old boy at presentation. 3D STIR only showed the primary mass in the left abdomen (white arrowheds) and no bone metastasis. DWI showed multiple bone lesions (black arrows) that were not confirmed on MIBG where only the abdominal mass was visible (black arrowheads).

due to the inhomogeneous or patchy signal of bone marrow, even in perfectly healthy subjects and can be a confusing factor [35] (Fig. 5).

We did not use ADC measurements of lesions on the DWI sequences, which could have increased the performance of the 3S protocol, particulary in oncological cases. However, ADC measurements have not yet been shown to discriminate, for example, between pathological and physiological lymphonodes with the same size [36].

There seems thus to be a controversy in paediatric literature concerning the utility of diffusion imaging and WBMRI. It would therefore be more cautious to suggest adding DWI to 3D STIR protocols for older children (not requiring sedation) for oncologic indications, until further studies confirm it's diagnostic yield based on more homogeneous populations.

Our study has other limitations: it includes patients with heterogeneous diseases (inflammatory, traumatic, neoplastic and hematological, both at onset and during the follow-up) and each group of disease has a low number of patients. Moreover, due to the small number of patients it was not possible to stratify our study group by patients weight and age, to evaluate their influence on diagnostic accuracy [17].

We do not have histological confirmation of lesions, because it was ethically impossible or simply not feasible in most cases.

Concerning the statistical analysis it has to be pointed out that only sensitivity and positive predictive value of the sequence are reported to quantify the diagnostic performance of 3D STIR. This is due to the fact that only positive findings can be enumerated exhaustively (free-response paradigm) while true negative findings are potentially infinite and thus impossible to consider in order to calculate specificity and negative predictive value.

5. Conclusions

Our findings raise many questions and suggest the need of further prospective studies. We found that WB-MRI performance depends on the pediatric radiology experience no matter which protocol was used (short or conventional). In conclusion, for a given radiologist, a short protocol does not seem to imply lower diagnostic performance. This is paramount for younger children in order to reduce sedation time and patient discomfort. Analysis of our data suggests that the non inferiority of 3D STIR should be confirmed by future studies stratifiying patients by pathology, weight and age.

Conflicts of interest

None.

Acknowledgements

The authors are grateful to Mr. Anderson Spartacus Aprigio for helping to collect the data for our research.

References

[1] R.A.J. Nievelstein, A.S. Littooij, Whole-body MRI in paediatric oncology, La Radiol. Med. 121 (5) (2016) 442–453.
[2] S. Toledano-Massiah, A. Luciani, E. Itti, P. Zerbib, A. Vignaud, K. Belhadj, L. Baranes, C. Haioun, C. Lin, A. Rahmouni, Whole-body diffusion-weighted imaging in hodgkin lymphoma and diffuse large B-Cell lymphoma, Radiographics 35 (3) (2015) 747–764.
[3] F. Bamberg, H. Kauczor, S.S. Weckbach, C.L. Schlett, M. Forsting, S.C. Ladd, K.H. Greiser, M. Weber, J. Schulz Menger, T. Niendorf, T. Pischon, S. Caspers, K Amunts, K. Berger, R.R.B. low, N. Hosten, K. Hegenscheid, T. Kröncke, J. Linseisen, M. Günther, J.G. Hirsch, A. Köhn, T. Hendel, H. Wichmann, B. Schmidt, K. Jöckel, W. Hoffmann, R. Kaaks, M.F. Reiser, H. Völzke, Whole-body MR imaging in the German National Cohort: rationale, design, and technical background, Radiology 277 (1) (2015) 206–220.
[4] A.S. Littooij, T.C. Kwee, I. Barber, C. Granata, M.A. Vermoolen, G. Enrlquez, J Zslros, S.Y. Soh, B. de Keizer, F.J. Beek, M.G. Hobbelink, M.B. Bierings, J. Stoker, R.A.J. Nievelstein, Whole-body MRI for initial staging of paediatric lymphoma: prospective comparison to an FDG-PET/CT-based reference standard, Eur Radiol. 24 (5) (2014) 1153–1165.
[5] A.M. Korchi, S. Hanquinet, M. Anooshiravani, L. Merlini, Whole-body magnetic resonance imaging: an essential tool for diagnosis and work up of

non-oncological systemic diseases in children. Minerva Pediatr. 66 (3) (2014) 169–176.
[6] M.B. Axelsen, I. Eshed, A. Duer-Jensen, J.M. Moller, S.J. Pedersen, M. Ostergaard, Whole-body MRI assessment of disease activity and structural damage in rheumatoid arthritis: first step towards an MRI joint count. Rheumatology (Oxford) 53 (5) (2014) 845–853.
[7] A. Ziobrowska Bech, B. Fiirgaard, C. Heuck, O. Ramsgaard Hansen, T. Herlin. Ten-year review of Danish children with chronic non-bacterial osteitis. Clin. Exp. Rheumatol. 31 (6) (2013) 974–979.
[8] T.C. Lauenstein, L.S. Freudenberg, S.C. Goehde, S.G. Ruehm, M. Goyen, S. Bosk, J.F. Debatin Jr., J. Barkhausen Jr., Whole-body MRI using a rolling table platform for the detection of bone metastases, Eur. Radiol. 12 (8) (2002) 2091–2099.
[9] D.L. Miglioretti, E. Johnson, A. Williams, R.T. Greenlee, S. Weinmann, L.I. Solberg, H.S. Feigelson, D. Roblin, M.J. Flynn, N. Vanneman, R. Smith Bindman, The use of computed tomography in pediatrics and the associated radiation exposure and estimated cancer risk, JAMA Pediatrics 167 (8) (2013) 700–707.
[10] M.S. Pearce, J.A. Salotti, M.P. Little, K. McHugh, C. Lee, K.P. Kim, N.L. Howe, C.M. Ronckers, P. Rajaraman, A.W. Sir Craft, L. Parker, A. Berrington de González, Radiation exposure from CT scans in childhood and subsequent risk of leukaemia and brain tumours: a retrospective cohort study, Lancet (London, England) 380 (9840) (2012) 499–505.
[11] V.L. Mango, E.A. Morris, D. David Dershaw, A. Abramson, C. Fry, C.S. Moskowitz, M. Hughes, J. Kaplan, M.S. Jochelson, Abbreviated protocol for breast MRI: are multiple sequences needed for cancer detection? Eur. J. Radiol. 84 (1) (2015) 65–70.
[12] R.M. Marks, A. Ryan, E.R. Heba, A. Tang, T.J. Wolfson, A.C. Gamst, C.B. Sirlin, M.R. Bashir, Diagnostic per-patient accuracy of an abbreviated hepatobiliary phase gadoxetic acid-enhanced MRI for hepatocellular carcinoma surveillance, AJR, Am. J. Roentgenol. 204 (3) (2015) 527–535.
[13] C.K. Kuhl, S. Schrading, K. Strobel, H. Schild, R. Hilgers, H.B. Bieling, Abbreviated breast magnetic resonance imaging (MRI): first postcontrast subtracted images and maximum-intensity projection-a novel approach to breast cancer screening with MRI, J. Clin. Oncol. 32 (22) (2014) 2304–2310.
[14] N. Barnea Goraly, S.A. Weinzimer, K.J. Ruedy, N. Mauras, R.W. Beck, M.J. Marzelli, P.K. Mazaika, T. Aye, N.H. White, L. Tsalikian, C. Kollman, P. Cheng, A.L. Reiss, High success rates of sedation-free brain MRI scanning in young children using simple subject preparation protocols with and without a commercial mock scanner?the Diabetes Research in Children Network (DirecNet) experience, Pediatr. Radiol. 44 (2) (2014) 181–186.
[15] C.J. Kellenberger, M. Epelman, S.F. Miller, P.S. Babyn, Fast STIR whole-body MR imaging in children, Radiographics 24 (5) (2004) 1317–1330.
[16] C.J. Kellenberger, S.F. Miller, M. Khan, D.L. Gilday, S. Weitzman, P.S. Babyn, Initial experience with FSE STIR whole-body MR imaging for staging lymphoma in children, Eur. Radiol. 14 (10) (2004) 1829–1841.
[17] M.J. Siegel, S. Acharyya, F.A. Hoffer, J.B. Wyly, A.M. Friedmann, B.S. Snyder, P.S. Babyn, G. Khanna, B.A. Siegel, Whole-body MR imaging for staging of malignant tumors in pediatric patients: results of the american college of radiology imaging network 6660 trial, Radiology 266 (2) (2013) 599–609.
[18] S. Punwani, S.A. Taylor, A. Bainbridge, V. Prakash, S. Bandula, E. De Vita, O.E. Olsen, S.F. Hain, N. Stevens, S. Daw, A. Shankar, J.B. Bomanji, P.D. Humphries, Pediatric and adolescent lymphoma: comparison of whole-body STIR half-Fourier RARE MR imaging with an enhanced PET/CT reference for initial staging, Radiology 255 (1) (2010) 182–190.
[19] K. Darge, D. Jaramillo, M.J. Siegel, Whole-body MRI in children: current status and future applications, Eur. J. Radiol. 68 (2) (2008) 289–298.
[20] M.A. Kwee, E.A. Vermoolen, M.J. Akkerman, R. Kersten, I. Fijnheer, F.J. Beck, M.B. van Leeuwen, M.C. Bierings, J. Bruin, H.M.E. Quarles van Ufford, J. de Klerk, J. Adam, C.S. Stoker, R.A.J. Nievelstein, Whole-body MRI, including diffusion-weighted imaging, for staging lymphoma: comparison with CT in a prospective multicenter study, J. Magn. Reson. Imaging 40 (1) (2014) 26–36.
[21] C. Lin, A. Luciani, E. Itti, T. El-Gnaoui, A. Vignaud, P. Beaussart, S.J. Lin, K.K. elhadj, P. Brugières, E. Evangelista, C. Haioun, M. Meignan, A. Rahmouni, Whole-body diffusion-weighted magnetic resonance imaging with apparent diffusion coefficient mapping for staging patients with diffuse large B-cell lymphoma, Eur. Radiol. 20 (8) (2010) 2027–2038.
[22] J. Gu, T. Chan, J. Zhang, A.Y. Leung, Y.L. Kwong, P.L. Khong, Whole-body diffusion-weighted imaging: the added value to whole-body MRI at initial diagnosis of lymphoma, AJR Am. J. Roentgenol. 197 (3) (2011) W384–91.
[23] M.H. Pui, S.K. Chang, Comparison of inversion recovery fast spin-echo (FSE) with T2-weighted fat-saturated FSE and T1-weighted MR imaging in bone marrow lesion detection, Skeletal Radiol. 25 (2) (1996) 149–152.
[24] S.A. Mirowitz, P. Apicella, W.R. Remus, A.M. Hammerman, MR imaging of bone marrow lesions: relative conspicuousness on T1-weighted, fat-suppressed T2-weighted, and STIR images, AJR, Am. J. Roentgenol. 162 (1) (1994) 215–221.
[25] M. Viallon, M.I. Vargas, H. Jlassi, K.O. Lövblad, J. Delavelle, High-resolution and functional magnetic resonance imaging of the brachial plexus using an isotropic 3D T2 STIR (Short Term Inversion Recovery) SPACE sequence and diffusion tensor imaging, Eur. Radiol. 18 (5) (2008) 1018–1023.
[26] T.C. Kwee, H.M. van Ufford, F.J. Beek, T. Takahara, C.S. Uiterwaal, M.B. Bierings, I. Ludwig, R. Fijnheer, R.A.J. Nievelstein, Whole-body MRI, including diffusion-weighted imaging, for the initial staging of malignant lymphoma: comparison to computed tomography, Invest. Radiol. 44 (10) (2009) 683–690.
[27] D.P. Chakraborty, A brief history of free-response receiver operating characteristic paradigm data analysis, Acad. Radiol. 20 (7) (2013) 915–919.
[28] J.M.J. Perez Rossello, S.A.S. Connolly, A.W.A. Newton, K.H.K. Zou, P.K.P. Kleinman, Whole-body MRI in suspected infant abuse, AJR, Am. J. Roentgenol. 195 (3) (2010) 744–750.
[29] M. Tanabe, H. Takahashi, N. Ohnuma, J. Iwai, H. Yoshida, Evaluation of bone marrow metastasis of neuroblastoma and changes after chemotherapy by MRI, Med. Pediatr. Oncol. 1 (1) (1993) 54–59.
[30] H.W. Goo, Whole-body MRI of neuroblastoma, Eur. J. Radiol. 75 (3) (2010) 306–314.
[31] N. Lebtahi, F. Gudinchet, M. Nenadov Beck, D. Beck, A. Bischof Delaloye, Evaluating bone marrow metastasis of neuroblastoma with iodine-123-MIBG scintigraphy and MRI, J. Nucl. Med. 38 (9) (1997) 1389–1392.
[32] T. von Kalle, N. Heim, T. Hospach, M. Langend¿rfer, P. Winkler, T. Stuber, Typical patterns of bone involvement in whole-body MRI of patients with chronic recurrent multifocal osteomyelitis (CRMO), RFo, Fortschritte auf dem Gebiet der Rntgenstrahlen und der bildgebenden Verfahren 185 (7) (2013) 655–661.
[33] N. Leclair, G. Thürmer, I. Sorge, L. Ritter, V. Schuster, F.W. Hirsch, Whole-body diffusion-weighted imaging in chronic recurrent multifocal osteomyelitis in children, PLoS One 11 (1) (2016) e0147523.
[34] J. Gu, T. Chan, J. Zhang, A.Y. Leung, Y. Kwong, P. Khong, Whole-body diffusion-weighted imaging: the added value to whole-body MRI at initial diagnosis of lymphoma, AJR, Am. J. Roentgenol. 197 (3) (2011) W384–W391.
[35] L. Ording Müller, D. Avenarius, O.E. Olsen, High signal in bone marrow at diffusion-weighted imaging with body background suppression (DWIBS) in healthy children, Pediatr. Radiol. 41 (2) (2011) 221–226.
[36] T.C. Kwee, T. Takahara, M.A. Vermoolen, M.B. Bierings, W.P. Mali, R.A.J. Nievelstein, Whole-body diffusion-weighted imaging for staging malignant lymphoma in children, Pediatr. Radiol. 40 (10) (2010) 1592–1602.